Air-sea gas transfer for two gases of different solubility (CO_2 and O_2)

A Rutgersson[1], A Andersson and E. Sahlée

Department of Earth Sciences, Uppsala University, Uppsala, Sweden

E-mail: anna.rutgersson@met.uu.se

Abstract. At the land-based marine measuring site Östergarnsholm in the Baltic Sea, the eddy covariance technique was used to measure air-sea fluxes of carbon dioxide and oxygen. High-frequency measurements of oxygen were taken with a Microx TX3 optode using the luminescence lifetime technique. The system gives reasonable oxygen fluxes after the limited frequency response of the sensor was corrected for. For fluxes of carbon dioxide the LICOR-7500 instrument was used. Using flux data to estimate transfer velocities indicates higher transfer velocity for oxygen compared to carbon dioxide for winds above 5 m/s. There are too few data for any extensive conclusions, but a least-square fit of the data gives a cubic wind speed dependence of oxygen corresponding to $k_{660} = 0.074U_{10}^3$. The more effective transfer for oxygen compared to carbon dioxide above 5 m/s is most likely due to enhanced efficiency of oxygen exchange across the surface. Oxygen has lower solubility compared with carbon dioxide and might be more influenced by near surface processes such as microscale wave breaking or sea spray.

1. Introduction

Air-sea exchange of various gases is important for many applications, i.e., in atmospheric chemistry, marine biology and climate. Fluxes of carbon dioxide are the subject of continuing experimental and theoretical interest due to the link with global climate. Air-sea exchange of carbon dioxide (CO_2) has the obvious importance for atmospheric concentration and thus the radiation budget. Oxygen (O_2) in the ocean is of crucial importance as it is strongly linked to both carbon and nitrogen cycles [1,2] and a key component in eutrophication. As O_2 is always present in the atmosphere at fairly constant concentrations, the atmosphere acts as a sink or source depending mainly on the processes in the water. Results from more than a decade of direct measurements using the eddy covariance technique (EC) of CO_2 in marine environments show that there are still many challenges needing to be addressed, both in terms of methodology and physical understanding of the exchange processes. Most marine EC data are taken from ships and Blomquist *et al*. [3] demonstrates experimental approaches for improving measurement precision and accuracy. Several of the problems are, however, avoided when taking the measurements on a land based stationary tower. In contrast to CO_2 there are very few existing studies using EC measurements for O_2, as the technique for applying fast response sensors is very new [4].

During recent decades much effort has gone into determining the relationship between the air-sea gas transfer velocity and different dynamical forcing processes, see e.g., Garbe *et al*. [5]. Gas transfer velocity describes the efficiency of the gas transfer across the interface. Over the years numerous laboratory and field studies have been conducted and several expressions suggesting relating the gas transfer to different physical variables, such as sea spray and bubbles [6, 7, 8, 9], surface films [10, 11],

Content from this work may be used under the terms of the Creative Commons Attribution 3.0 licence. Any further distribution of this work must maintain attribution to the author(s) and the title of the work, journal citation and DOI.
Published under licence by IOP Publishing Ltd

water-side convection [12, 13] and rain [14]. Still wind speed is the most robust single parameter to describe the transfer velocity. The relative importance of these processes for air-sea exchange is likely to vary for gases of different solubility and is still not fully understood [5]. It is well known that water vapour and heat (corresponding to very high solubility) have less wind speed dependence than CO_2 (e.g., [15]), acetone with high solubility [16] has a smaller wind speed dependence. O_2 has a lower solubility than CO_2, but is frequently assumed to follow the same wind speed dependence. Previous estimates of the transfer velocity of O_2 are determined using a budget method [17] or eddy covariance fluxes in the water [18].

We here use data taken using the EC method of carbon dioxide and oxygen at the land based site Östergarnsholm. By simultaneously using gases of different solubility we expect to expand knowledge on the important processes for transfer velocities of gases in general. Few previous studies exist using EC measurements of oxygen in the atmosphere. Andersson *et al*. [4], however, show the potential of using a high-frequency probe, based on a luminescence lifetime technique.

2. Methods and data

2.1. Theory

Air-sea fluxes of gases (F) are typically calculated from concentration gradients in either the air side or water side using the two-layer model [19]:

$$F = K_a(\frac{C_w}{H} - C_a) = K_w(C_w - HC_a) \quad (1)$$

C_w and C_a are the gas concentrations in bulk water and air, H is the dimensionless Henrys solubility. The total gas transfer velocity from the perspective of the air-side gradient (K_a) or water-side concentration gradient (K_w) are related by $K_a = HK_w$. The total gas transfer velocities are composed of the individual transfer velocities in the air phase and water phase (k_a and k_w, respectively).

$$K_a = \frac{1}{(1/k_a + 1/Hk_w)}; \quad K_w = \frac{1}{(1/k_w + 1/Hk_a)} \quad (2)$$

CO_2 and O_2 are both gases with low solubility and thus water-side controlled (i.e., $K_w \approx k_w$), we here denote the total gas transfer velocity k and assume it to be equal to the water-side transfer coefficient of the gas. Rewriting equation 1 in terms of the gas partial pressure we get

$$k = \frac{F}{K_0 \Delta pC} \quad (3)$$

where K_0 is the gas specific solubility constant and ΔpC the air-sea difference of the partial pressure.

2.2. Site

The measurements used in this study are taken at the Östergarnsholm site in the Baltic Sea. This station is located at 57°27'N, 18°59'E (see figure 1). The site has been running semi-continuously since 1995; it is a land-based 30-m tower situated on the southern tip of a very small, flat island in the Baltic Sea. Flux of a quantity measured at a particular height is influenced by the surface conditions at a certain distance upwind; this area of influence is called the flux footprint. The relative role of upwind areas (flux footprint) can be estimated by applying expressions originally developed for atmospheric dispersion. For wind directions 80°<WD<210°, the data have been shown to represent open sea conditions, in the sense that the wave field is mainly undisturbed and the atmospheric turbulence and the fluxes of momentum, sensible heat, and latent heat are not influenced by either the limited water depth or the coast [21]. In Rutgersson *et al*. [20] CO_2 measurements were investigated, showing that for

wind from the 80°<WD<160° sector, the sensor for pCO_{2w} (partial pressure of CO_2 in the water) represents the footprint of the tower. The present investigation uses only data for winds from the 80°<WD<160° sector.

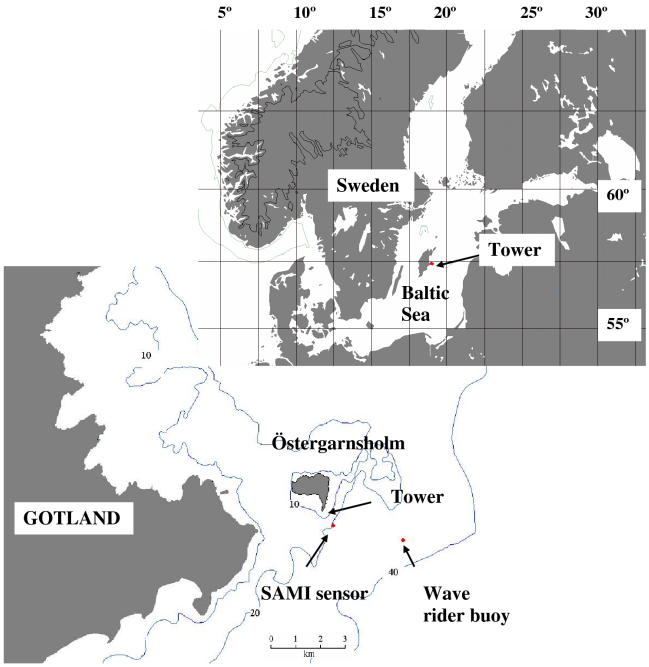


Figure 1. Map of the Östergarnsholm measurements site (from [20]). Positions of the tower and SAMI sensor are indicated by arrows. Thin solid lines represents iso-lines of water depth.

The tower is equipped with high-frequency instrumentation for turbulence measurements and slow-response sensors for mean profile measurements. High-frequency wind components are measured with CSAT3 (Campbell Scientific, North Logan, Utah, USA) sonic anemometers at three levels, i.e., 9, 16.5, and 25 m above the tower base, for earlier data the SOLENT 1012R2 sonic anemometers (Gill Instruments, Lymington, UK) were used. Sea level varies slightly, but the tower base is generally 1±0.5 m above mean sea level. The site and instrumentation protocols are further described in Rutgersson *et al*. [20]. The sampling rate of the eddy covariance system was set to 20 Hz and fluxes were calculated over 60-min intervals. There was careful quality control for all individual flux data points.

2.3. CO_2 data

The humidity and CO_2 fluctuations are measured with a LICOR-7500 (LICOR-Inc., Lincoln, NE, USA) open-path analyzer at 9 m above the tower base. For pCO_{2w} and sea surface temperature (SST) a SAMI sensor (Sunburst Sensors, Missoula, USA) is used [22]. It measures at a depth of approximately 4 m, 1 km SE of the tower (see figure 1). The investigated area is a sink or source of atmospheric CO_2 depending on the season, pCO_{2w} displays a significant seasonal cycle with summertime values of 150 µatm and up to 800 µatm in winter. A smaller seasonal cycle is observed in the atmosphere, with a peak-to-peak amplitude of 17 µatm [23]. The air-sea difference in partial pressure is relatively large (of the order of 50–200 µatm).

2.4. O_2 data

The high-frequency oxygen data were measured at the height of 25 m with the commercially available optode system Microx TX3 (PreSens- Precision Sensing GmbH, Regensburg, Germany). The Microx TX3 sampling rate is 2 Hz with a precision of 0.1% air saturation. The sensor was, however, found to have a limited response time, yielding a flux loss in the frequency range $f > 0.3$ Hz. This is corrected for by applying cospectral similarity simultaneously using measurements of latent heat as the reference

signal. On average the magnitude of the cospectral correction added 20% to the uncorrected oxygen flux (see [4] for details of the system and corrections). The measured fluxes were also density corrected according to Webb *et al*. [24], a significant term, sometimes also changing the direction of the fluxes. Figure 2 shows the set-up of the system with the CSAT3 sonic (figure 2a), the LICOR at the same height (figure 2b), and the needle of the oxygen sensor (figure 2c).

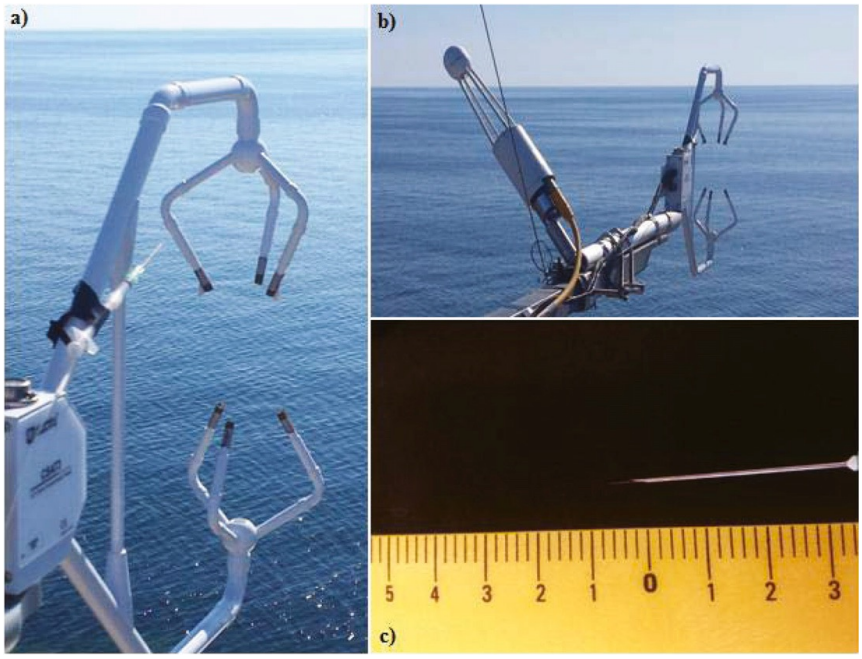


Figure 2. (a) The EC system with a close-up of the oxygen sensor mounted at the CSAT3, (b) the EC system at the height of 25 m, and (c) a close-up of the oxygen sensor tip. Figure from [4].

The water-side oxygen is measured by a SBE-43 sensor integrated on a SBE 37 smp-ido (Seabird Electronics Inc., Bellevue, Washington, USA) at 4 m depth placed at the mooring of the SAMI.

3. Results

3.1. Case study

During a field campaign in June 2013 fluxes of CO_2 and O_2 were measured simultaneously. The campaign was from June 19 to June 24 and the conditions are shown in figure 3. The data are characterized by three periods, the second period, 21 June to 23 June (decimal month 6.69 to 6.74), represents an upwelling period. The wind increases and the direction changes to 200° for more than 30 hours, this is typical for upwelling situations in this region [25]. The upwelling is also clearly seen in satellite SST maps for the period (not shown). As the buoy measurements are not representative for the flux footprint of the tower during the upwelling situation, these data are not used in the analysis of transfer velocity and the focus is on the first and third periods. The first period shows positive (upward directed) oxygen fluxes of 0.6–6.4 µmol m^{-2} s^{-1}, in agreement with the oxygen saturation in water varying between 105–108% (in figure 3 oxygen partial pressure is presented). After the upwelling period, oxygen saturation increases from 5% supersaturation to leveling off at 10% supersaturation when the water temperature goes back to 14°C during the third period and the oxygen fluxes are 0.35–-3 µmol m^{-2} s^{-1}. The partial pressure of CO_2 is significantly lower in the water compared to air, ΔpCO_2>150 µatm, indicating large fluxes and a large signal-to-noise ratio of the data.

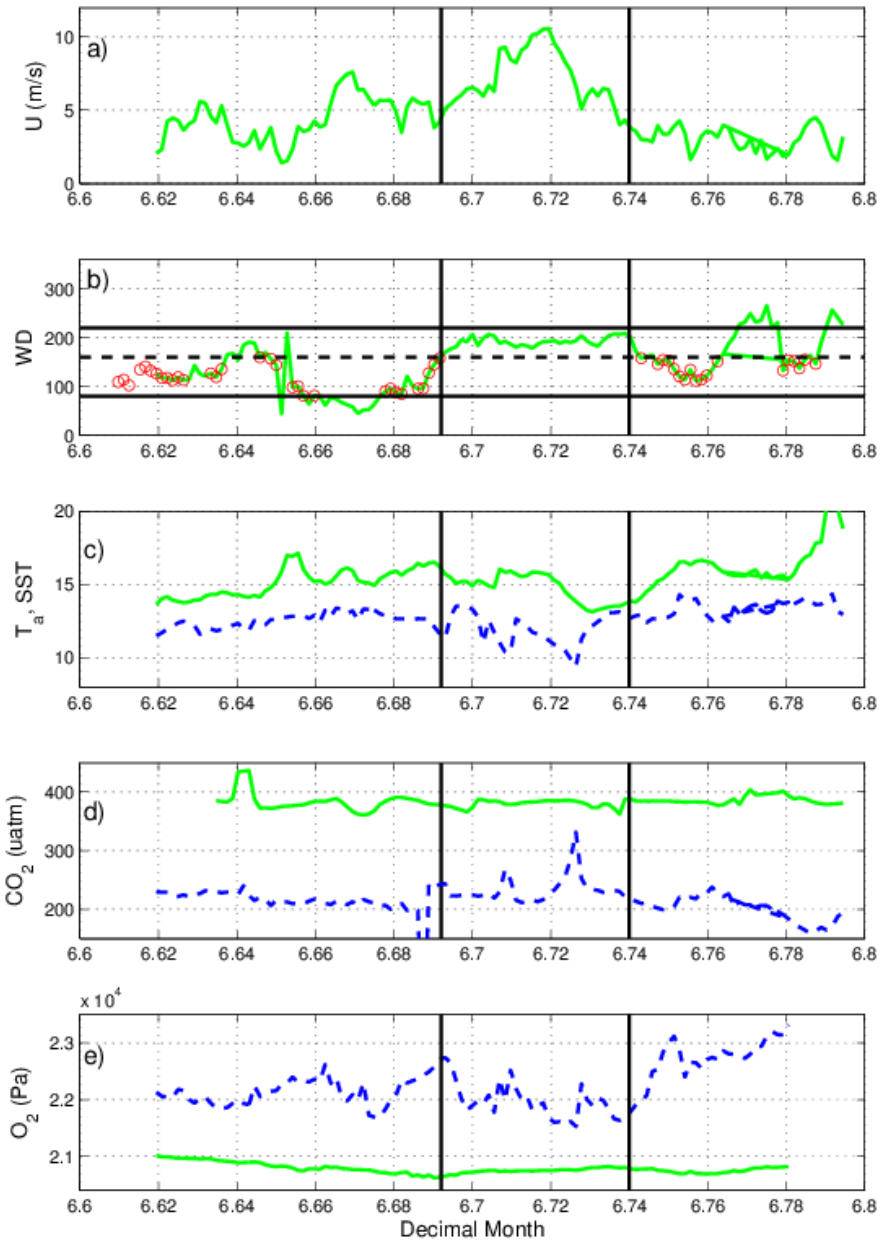


Figure 3. Field campaign June 19 to 24, 2013. Wind speed (a), wind direction (b), temperature (c), partial pressure of CO_2 (d) and O_2 (e). Green lines correspond to data taken in the tower and blue (dashed) curves to measurements in the water. Vertical black lines represent an upwelling period and horizontal black lines in (b) indicate the wind directions where measurements in the water are representative for conditions at the tower (these data are also shown by red circles).

Using the fluxes measured with the EC method and the air-sea differences of partial pressure the transfer velocities can be calculated according to equation 3. The transfer velocities of CO_2 and O_2 (denoted k_{660} when normalized to a Schmidt number of 660) are shown for various wind speeds in figure 4a. Shown also is the wind speed dependent equation $k_{660} = 0.26U_{10}^2$ derived for CO_2, where U_{10} is the wind speed at 10 m.

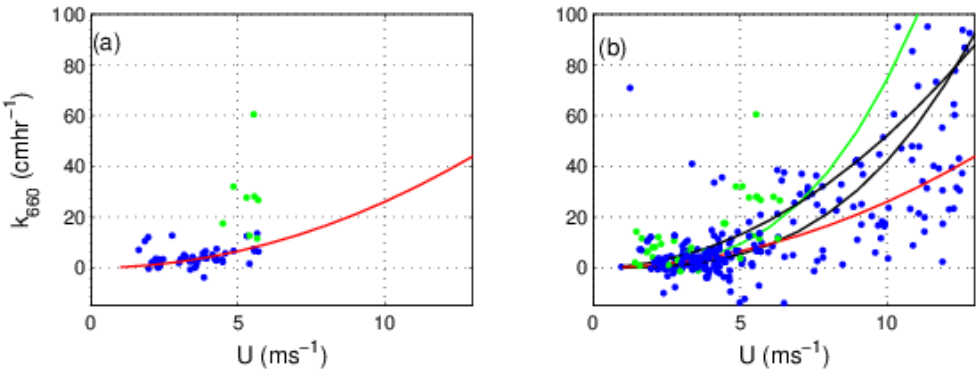


Figure 4. Transfer velocity of CO_2 (blue dots) and O_2 (green dots) for varying wind speeds for the field campaign (a) and for the extended data set (b). Red lines represent the wind speed dependent equation $k_{660} = 0.26U_{10}^2$. In (b) and green curve is $k_{660} = 0.074U_{10}^3$ and black lines represent expressions for O_2 from [17], corresponding to cubic (dashed) and quadratic (solid) equations, respectively.

There are few data for the oxygen transfer velocity and significant scatter, but the significantly higher values of k_{660} for O_2 compared to k_{660} for CO_2 for the same wind speeds indicate a more efficient transfer across the surface for the gas with the lower solubility. Both gases here experience the same environmental conditions because the measurements were taken simultaneously.

3.2. Extended data set

For a more extended analysis, several data sets are used. For CO_2 this includes data from 2005–2007 described in [12] as well as more recent data from 2013–2014, for O_2 this includes data from July 2011 and September 2011 in addition to June 2013. All data are taken at the Östergarnsholm site. Situations with water-side convection (defined as in [13]) have been removed as these data represent different conditions and no data exist for O_2 during such conditions. Figure 4b shows the transfer velocities of CO_2 and O_2 and the extended data set supports the case study. The data of O_2 are too few to draw any final conclusion, but figure 4 indicates a stronger wind speed dependence of O_2 than CO_2. A fit to the O_2 data points indicates a cubic wind speed dependence $k_{660} = 0.074U_{10}^3$ (shown by the green line in figure 4b), the O_2 transfer velocity is larger than for CO_2 at winds approximately larger than 5 m/s. Also shown are the two curves derived for O_2 in [17] using a cubic and quadratic wind speed dependence ($k_{660} = 0.042U_{10}^3$ and $k_{660} = 0.52U_{10}^2$, respectively). For CO_2 the scatter increases with increasing winds and for winds above 8 m/s some of the data points are well above the expected quadratic wind speed dependence (the red curve).

4. Discussion

For winds within the regime 5–7 m s^{-1} the measured transfer velocity for O_2 shows a stronger wind speed dependence than for CO_2 and also stronger compared to previous parameterizations developed for O_2. The resistance to transfer of gases of relatively low solubility across the sea surface can be seen as resistances in an electric circuit (e.g., [13]) and different processes are of different relative importance depending of the solubility of the gas. It is likely that processes enhancing the exchange more effectively for gases with a lower solubility starts to be of importance already at these wind speeds. Examples of such processes that could be active for our data are microscale wave breaking, bubbles or sea spray. The onset of breaking waves and whitecap coverage are generally found at lower wind speeds for coastal regions and marginal seas, which could explain the strong wind dependence at 5 m s^{-1}. The short averaging time scale in the EC method (here 60 min) makes it possible to relate the measured transfer velocity to episodic high wind events and to study the impact of processes acting on higher temporal resolution.

In Kihm and Körtzinger [17], the importance of high wind speeds for air-sea gas exchange of O_2 was pointed out when suggesting their cubic relation (giving significantly lower transfer velocities compared to our measurements). It is, however, likely that the effect from enhanced mixing with short time scales on the oxygen transfer velocity in [17] were underestimated as their results are based on a budget method with a much longer averaging time scale (7 days). Also for CO_2 the scatter at winds above 8 m/s can probably be explained by the presence of processes enhancing the efficiency of the mixing for some of the data.

5. Conclusions

High-frequency measurements of oxygen were taken with a Microx TX3 optode using a luminescence lifetime technique; the system gives reasonable oxygen fluxes after correcting for the limited frequency response. Using flux data to estimate the transfer velocity for oxygen indicates a higher transfer velocity for O_2 compared to CO_2 for winds above 5 m/s. There are too few data for extensive conclusions, but a least-square fit of the data gives a cubic wind speed dependence corresponding to $k_{660} = 0.074U_{10}^3$. The more effective transfer for O_2 compared to CO_2 above 5 m/s is most likely due to enhanced efficiency of air-sea transfer of O_2 with lower solubility due to microscale breaking or sea spray.

References

[1] Arrigo K R 2004 *Nature* **437** 349
[2] Keeling R F *et al* 2010 *Mar. Sci.* **2**
[3] Blomquist B W *et al* 2014 *Bound. Layer Meteorol*. **152** 245
[4] Andersson A *et al* 2014 *J. Atmos. Ocean. Technol*. **31** 2498
[5] Garbe C S *et al* 2014 *Ocean-Atmosphere Interactions of Gases and Particles* eds P Liss and M Johnson (Springer-Verlag) 55-112
[6] Monahan E C and Spillane M C 1984 *Gas Transfer at Water Surfaces* eds W Brutsaert and G H Jirka (Spinger-Verlag) 495–503
[7] Wallace D W R and Wirick C D 1992 *Nature* **356** 694
[8] Woolf D K *et al* 2007 *J. Mar. Syst.* **66** 71
[9] Asher W E and Wanninkhof R 1998 *J. Geophys.Res.* **103** 10555
[10] Frew N M 1997 *The Sea Surface and Global Change* eds P S Liss and R A Duce (Cambridge University Press) 121–72
[11] Salter M *et al* 2011 *J. Geophys. Res.* **116** C11016
[12] Rutgersson A and Smedman A 2010 *J. Mar. Syst*. **80** 125
[13] Rutgersson A *et al* 2011 *Geophys. Res. Lett*. **38** L02602
[14] Takagaki N and Komori S 2007 *J. Geophys. Res*. **112** C06006
[15] Rutgersson A *et al* 2001 *Bound.-Layer Meteor*. **99** 53
[16] Yang M *et al* 2014 *J. Geophys. Res.* **119** 7308
[17] Kihm C and A Körtzinger 2010 *J. Geophys. Res*. **115** C12003
[18] McNeil C D and D'Asaro E 2007 *J. Mar. Syst*. **66** 110
[19] Liss P S and P G Slater 1974 *Nature* **247** 181
[20] Rutgersson A M *et al* 2008 *J. Mar. Syst.* **74** 381
[21] Högström U *et al* 2008 *Boreal Environ. Res*. **13** 475
[22] DeGrandpre M *et al* 1995 *Limnol. Oceanog*. **40** 969
[23] Rutgersson A *et al* 2009 *Bor. Environ. Res.* **14** 238
[24] Webb E K *et al* 1980 *Q. J. R. Meteorol. Soc*. **106** 85
[25] Norman M *et al* 2013 *Tellus* B **65**